Estimating deer density and abundance using spatial mark–resight models with camera trap data

Andrew J. Bengsen,[1,*] , David M. Forsyth,[1] Dave S. L. Ramsey,[2] Matt Amos,[3] Michael Brennan,[3] Anthony R. Pople,[3] Sebastien Comte,[1] and Troy Crittle[4]

[1]*NSW Department of Primary Industries, Vertebrate Pest Research Unit, 1447 Forest Road, Orange, NSW 2800, Australia*
[2]*Arthur Rylah Institute for Environmental Research, Department of Environment, Land, Water and Planning, 123 Brown Street, Heidelberg, VIC 3084, Australia*
[3]*Queensland Department of Agriculture and Fisheries, 41 Boggo Road, Dutton Park, QLD 4102, Australia*
[4]*NSW Department of Primary Industries, Biosecurity and Food Safety, 4 Marsden Park Road, Calala, NSW 2340, Australia*

*To whom correspondence should be addressed: andrew.bengsen@dpi.nsw.gov.au

Globally, many wild deer populations are actively studied or managed for conservation, hunting, or damage mitigation purposes. These studies require reliable estimates of population state parameters, such as density or abundance, with a level of precision that is fit for purpose. Such estimates can be difficult to attain for many populations that occur in situations that are poorly suited to common survey methods. We evaluated the utility of combining camera trap survey data, in which a small proportion of the sample is individually recognizable using natural markings, with spatial mark–resight (SMR) models to estimate deer density in a variety of situations. We surveyed 13 deer populations comprising four deer species (*Cervus unicolor, C. timorensis, C. elaphus, Dama dama*) at nine widely separated sites, and used Bayesian SMR models to estimate population densities and abundances. Twelve surveys provided sufficient data for analysis and seven produced density estimates with coefficients of variation (CVs) ≤ 0.25. Estimated densities ranged from 0.3 to 24.6 deer km^{-2}. Camera trap surveys and SMR models provided a powerful and flexible approach for estimating deer densities in populations in which many detections were not individually identifiable, and they should provide useful density estimates under a wide range of conditions that are not amenable to more widely used methods. In the absence of specific local information on deer detectability and movement patterns, we recommend that at least 30 cameras be spaced at 500–1,000 m and set for 90 days. This approach could also be applied to large mammals other than deer.

Key words: abundance, capture–recapture, Cervidae, detection rate, fallow deer, population estimation, red deer, rusa deer, sambar deer

Reliable estimates of population size or density are needed for wildlife research and management (Williams et al. 2002). This is especially true for deer (family: Cervidae), which have a wide-ranging global distribution (Mattioli 2011) and are often subject to intensive population management such as controlled harvesting or culling (McShea et al. 1996; Hewitt 2011). A wide range of methods have been used to estimate deer abundance (*N*) and density (*D*). The relative use of each method has varied regionally and temporally. Counts of deer or their sign from terrestrial or aerial transects have been most common in recent years (Forsyth et al. 2022). However, the use of camera traps for deer surveys has increased since the 2000s, particularly in North America (Forsyth et al. 2022). Camera trap surveys are particularly well-suited to habitats with dense canopy

cover in which the detection probability of methods such as terrestrial or aerial transects are typically too low to be useful (Gardner et al. 2019).

Spatial capture–recapture is a common approach to estimating abundance and density from camera trap images (Efford and Fewster 2013; Royle et al. 2013). Spatial capture–recapture methods require a large proportion of detected animals to be consistently identifiable as individuals by natural or anthropogenic marks (Royle et al. 2013; Parsons et al. 2017). However, capturing deer to apply markings such as ear tags or tracking collars can be expensive, logistically challenging, and can compromise the health and survival of captured animals (Hampton et al. 2019; Bengsen et al. 2021). Capture and marking can also induce bias in estimators if the sample of marked animals is not

representative of the broader population of interest (Royle et al. 2013). Most deer species are characterized by a high proportion of nondescript individuals and it is often the case that too few naturally marked and identifiable deer are detected for spatial capture–recapture methods to be applicable (see below).

Spatial mark–resight (SMR) models (Royle et al. 2013; Sollmann et al. 2013a) can overcome some of the above limitations by combining detection information from a small proportion of individually identifiable (i.e., "marked") individuals with information on unidentifiable (i.e., "unmarked") individuals. These models use the locations of detections from marked and unmarked animals to estimate the number and location of activity centers. Using this information, SMR models estimate *N* within a defined state space that is usually larger than the area that was surveyed (Chandler and Royle 2013; Royle et al. 2013). SMR models and camera traps have been used to estimate carnivore population densities (e.g., Rich et al. 2014; Kane et al. 2015; Forsyth et al. 2019) and have proven useful for some ungulates (e.g., Jiménez et al. 2017; Gardner et al. 2019). However, only one study has evaluated the applicability of estimating *N* or *D* using camera traps with SMR methods for any species of deer (Macaulay et al. 2019). That study showed that the approach was useful for estimating the density of one temperate deer species at a single site using an ad hoc sampling design. Further studies that apply a systematic and repeatable sampling design to survey a range of species characterized by different spatial and social behaviors and occupying a wider range habitat types are desirable for a more robust evaluation of the method.

Estimates of *N* or *D*, termed $\hat{N}$ or $\hat{D}$, are subject to sampling error. The precision of estimates is often compared using the coefficient of variation (CV), which is the ratio of the sample variability to the estimated value (Skalski et al. 2005). A CV of ≤0.25 is sometimes considered desirable for $\hat{N}$ or $\hat{D}$ (Skalski et al. 2005; 500–501), but the required CV will depend on the use of the estimates. A survey aiming to detect a small change in $\hat{N}$ or $\hat{D}$, for example, will need greater precision than one aiming to detect a larger change. A recent review reported that most (72%) published deer abundance and density estimates did not report precision, and only 26% of those that did reported a CV ≤ 0.25 (Forsyth et al. 2022).

In this paper, we report the application of SMR models to estimate $\hat{D}$ from camera trap surveys of four deer species at nine sites in eastern Australia. Deer were deliberately introduced into Australia to establish populations for hunting, but some populations have established from escaped farm animals (Moriarty 2004a). Knowing the abundance and density of wild deer populations in Australia is important for management, both as a hunting resource and to minimize their adverse impacts (Moriarty 2004a; Davis et al. 2016). The sites at which we conducted our study ranged from temperate to tropical and from coastal to montane. The breadth of study area shapes, sizes, habitats, and deer species provide a powerful test of SMR methods for estimating deer abundance and density. Our objective was to evaluate the utility of SMR models for estimating $\hat{D}$ in deer populations and the levels of precision obtained under diverse real-world situations. Finally, we provide recommendations for the use of SMR to estimate the abundance and density of deer.

Materials and Methods

Camera trap surveys.—Deer species, topography, vegetation, and site size varied among sites, but we used the same key principles to guide survey design throughout the study. We overlaid each of nine survey sites (Fig. 1) with a hexagonal grid and deployed a camera within a 50-m radius around the centroid of each grid cell. This provided an approximately even spacing among neighboring cameras, while allowing us to position cameras on game trails and other features that would enhance the probability of detecting deer that were using the area around the grid cell centroid. We avoided features such as ponds and large clearings that were not representative of, or pervasive throughout, the area close to the cell centroid. In this way, we sought to obtain a larger sample of individuals spread across each study site than would have otherwise been possible, while minimizing bias in our estimates due to targeted or convenience sampling. The distance between centroids varied among sites, ranging from 300 to 800 m. This spacing ensured that individual deer had the potential to be encountered at several camera locations, thereby creating spatial correlation in individual detection histories. We positioned a marker post 6 m in front of the camera to delimit a standardized detection zone and only analyzed deer detections within that field of view. To avoid the risk of modifying deer behavior and introducing an uncontrolled source of bias to our estimates, no baits or lures were used to attract animals to the camera. We used Reconyx HC600 cameras (Reconyx LLP, Holmen, Wisconsin) at all sites, unless specified otherwise. Cameras were set horizontally on trees or posts, aimed approximately 40 cm above ground level on the post 6 m from the camera. We set all cameras to record a burst of five images in immediate succession for each camera trigger event, with no mandatory elapsed time between subsequent trigger events. We used a 2- to 3-month survey period at each site to strive for a sample size that would provide favorable precision and low bias. Simulation studies have suggested that survey durations of between 2 and 5 months should optimize precision and bias of spatial capture–recapture estimates in species with intermediate life histories (DuPont et al. 2019). Surveys at each site were timed to avoid seasons when spatial behavior was likely to be unstable (e.g., rutting seasons for fallow and red deer). None of the populations we surveyed were expected to experience intense seasonal mortality or movement (e.g., due to hunting seasons or migration) that would violate the assumption of population closure.

Study sites.—The nine study sites varied in their geographic characteristics, deer species present, and sampling intensity (Table 1). Sites CD (145.41, −37.96), SL (145.31, −37.67), and YY (145.15, −37.4) were water supply reservoirs in the hills around Melbourne, Victoria. A large water body and a tall (approximately 2.4 m high) deer-resistant mesh fence provided hard inner and outer boundaries at these three sites (Fig. 2).
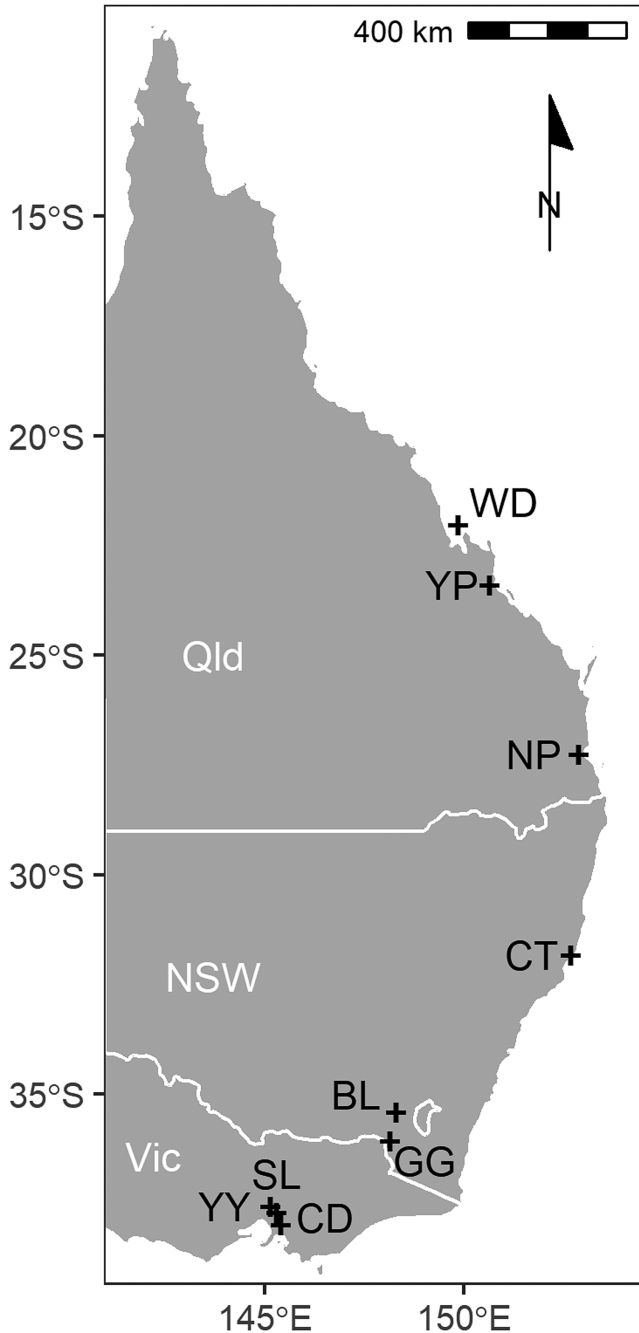
Fig. 1.—Location of nine study sites in the states of Queensland, New South Wales, and Victoria, eastern Australia.

These boundaries defined the state space and ensured geographic closure over the sampling area. The survey was conducted during the 2017/2018 austral summer.

Sites GG (148.13, −36.04) and BL (148.32, −35.40) were located inside Kosciuszko National Park in southeast New South Wales. The state space was defined by a 3-km buffer around the outer cameras, trimmed to exclude large expanses of treeless farmland at both sites and a large water body at BL (Fig. 2). These areas were excluded because they were not representative of the heavily wooded survey areas and did not provide habitat that was likely to support activity range centers for sambar or fallow deer. The buffer distance was selected to balance computational speed and the requirement that deer with activity centers beyond the state space would not appear on the survey grid. Surveys were conducted during the 2018/2019 austral summer.

Sites YP (150.66, −23.39) and WD (149.87, −22.00) were in coastal central Queensland and site NP (152.89, −27.24) was a water supply reservoir in southeast Queensland. WD was a small uninhabited island approximately 22 km from the mainland. Deer populations at YP and WD were targeted for eradication by local or state management agencies. A grid of Swift 3C cameras (Outdoor Cameras Australia, Toowoomba, Queensland, Australia) was used at each site. Cameras at YP were deployed between May and August 2019 and those at WD and NP were deployed between August and October 2019. The state space at YP was defined by a 3-km buffer around the outer cameras, whereas the NP state space was defined by a 1.5-km buffer which was trimmed to remove the reservoir. The high tide mark provided a hard boundary at WD (Fig. 2).

Site CT (152.67, −31.81) was a wetland reserve in coastal New South Wales. The resident sambar deer population was targeted for eradication by the local council. One rusa deer was also photographed at one camera trap. Due to the two species' ability to hybridize (Martins et al. 2018) and difficulties in consistently discriminating between them using camera trap images, the single deer detection that was identified as rusa by antler morphology was included in the sambar data set. A grid of 31 HS2X cameras (Reconyx LLP, Holmen, Wisconsin) was deployed during the 2018/2019 austral summer. The state space was defined by a 3-km buffer around the outer cameras, trimmed of open agricultural land and human settlements (Fig. 2).

Table 1.—Site and survey characteristics for 13 deer density estimation surveys. Area is the area of the hexagonal grid used to site cameras at sites with permeable boundaries or the area enclosed by fences or water for sites with impermeable boundaries (denoted by †).

Site	Deer species	Vegetation	Terrain	Cameras	Area (km²)	Days	Camera spacing (m)
SL†	Red, Sambar	Woodland	Undulating	12	4.7	108	800
YY†	Red, Sambar	Woodland	Undulating	29	14.6	109	800
CD†	Fallow, Sambar	Woodland	Undulating	31	12.3	109	800
GG	Fallow, Sambar	Woodland, forest	Montane	39	8.4	89	500
BL	Sambar	Woodland, forest	Montane	40	8.7	89	500
CT	Sambar	Wetland, forest	Flat	31	13.2	89	700
NP	Rusa	Woodland	Undulating	35	7.6	58	500
YP	Rusa	Woodland	Hilly	36	2.8	79	300
WD†	Rusa	Woodland, forest	Undulating	44	3.8	64	300
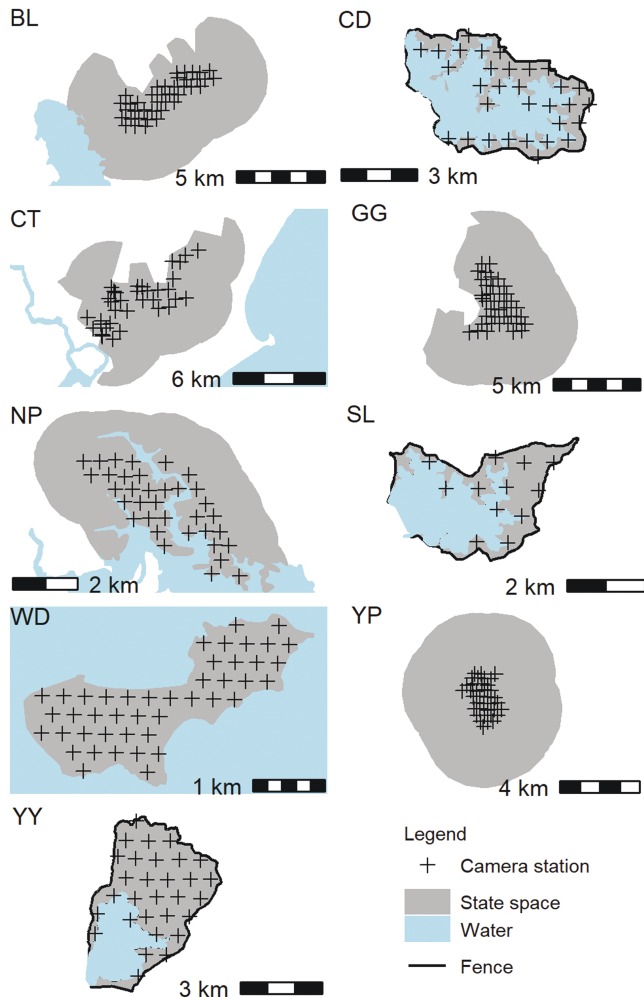
**Fig. 2.**—Camera station and state space configuration at each of nine deer survey sites.

Density estimation.—The data used to estimate density included the camera trap spatial coordinates and spatial detection histories for recognizable (marked) individuals and unrecognizable (unmarked) deer. We inspected camera trap images and appended additional metadata using Exifpro (Kowalski and Kowalski 2013). We grouped consecutive photos into the same event if they were separated by <10 min from the next series of photos of the same species. We selected this interval by inspecting the distribution of times between successive camera triggers for all combinations of species and site, which showed that most (55%) camera triggers caused by deer occurred within 10 min of the previous deer trigger event and the remaining times between consecutive deer triggers were spread sparsely between 10 min and 78 days (Supplementary Data SD1). Variables recorded included: (i) the species within the image, (ii) the minimum number of deer that passed through the 6-m detection zone during the event, (iii) the minimum number of deer within the entire field of view, and (iv) the individual identification codes for deer that could be recognized as distinct individuals within the detection zone.

We only used naturally occurring markings to identify deer. We were careful to avoid relying on ambiguous markings when assigning individual identification codes for deer so that

we reduced the risk of failing to recognize subsequent recaptures. Such a failure would lead to the underestimation of detection probability and overestimation of density (Evans and Rittenhouse 2018). When assigning an initial identification, observers considered whether markings were sufficiently obvious that any trained observer would be able to recognize the same individual at a different camera and time, including at night under infrared illumination. Animals were not assigned an individual identification code unless markings were clear and obvious from multiple camera angles. Image brightness and contrast were sometimes altered using Exifpro to enhance the visual clarity of markings. Markings used for individual recognition included obvious antler shapes and deformations, distinctive scarring on both sides of the body, and limb deformations that were unlikely to greatly hinder mobility and introduce bias into the estimation of movement patterns (Fig. 3). All individuals at a given site were identified by a single experienced observer.

We extracted metadata from camera trap images and constructed detection histories for the marked and unmarked components of our samples using the camtrapR package (Niedballa et al. 2016) in the R statistical computing environment (R Core Team 2020). Detection histories for marked animals comprised a three-dimensional array of each individual's history of detection or nondetection at each camera station on each day. Many deer showed markings that might enable them to be identified as individuals in different sequences of images, but our conservative identification guidelines meant that fewer than 10 individuals were assigned at most sites. Unmarked detection histories comprised a matrix of the number of detections at each camera on each day.

We fitted Bayesian SMR models using Metropolis-within-Gibbs MCMC algorithms (adapted from Chandler and Royle 2013; Royle et al. 2013; Sollmann et al. 2013a; Ramsey et al. 2015) implemented in R to estimate the density of each deer species present at each site. SMR models combine spatially explicit observation models for marked and unmarked animals with a point process model that estimates the spatial distribution of the activity centers of animals. In the observation models, the probability of detecting an animal at a camera station is assumed to follow a decreasing function of distance between the camera and the animal's activity center. The detection function is estimated from spatiotemporal variation in detection histories which provide repeated spatial distances between detections and putative activity centers. Detection histories for marked and identifiable animals are fully observed, but the number of individuals that are never detected is unknown and thus estimated using parameter-expanded data augmentation (DA). For DA, the marked detection histories are augmented with an arbitrarily large number of pseudo-individuals that are never detected. A Bernoulli sampling process with probability of success ψ is used to determine whether each pseudo-individual represented an animal that was present but not detected (Royle et al. 2013). The location of the activity center for each unmarked individual within the survey area is inferred from the spatial correlation of unmarked detections, assuming a similar observation model to that estimated from
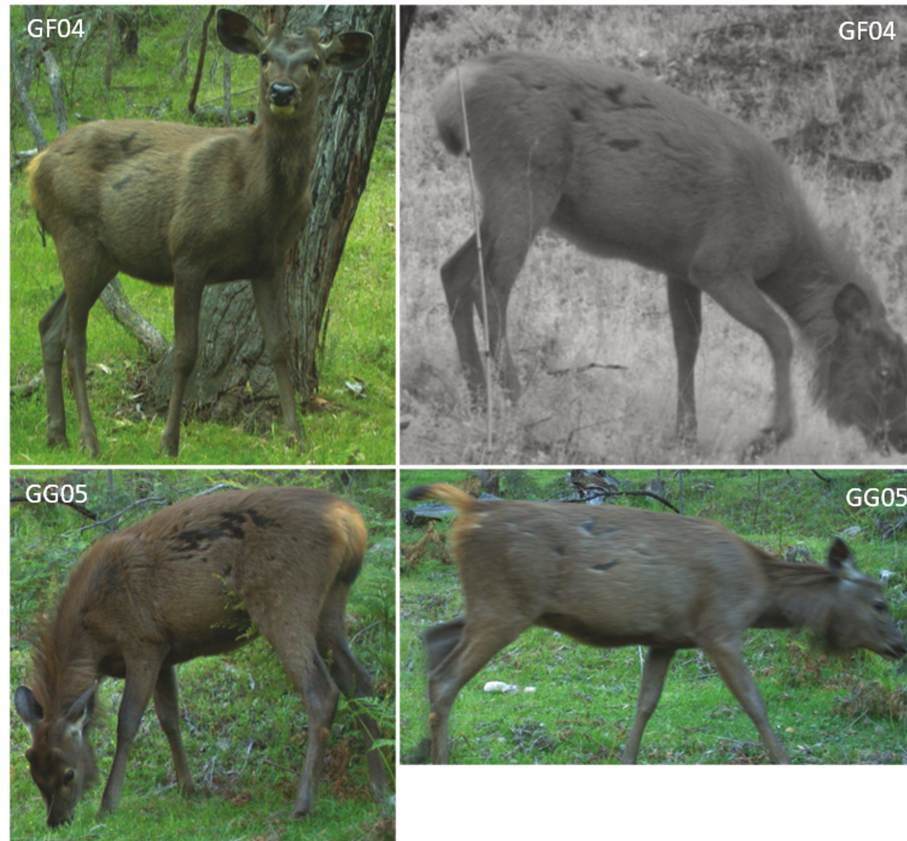
Fig. 3.—Representative images of sambar deer S_GF04_001 taken from four occasions at two adjacent camera trap stations (GF04, GG05) showing distinctive and consistently observable scarring on both sides of the body.

the marked individuals. The number of unmarked activity centers is again estimated using DA. The process model assumes that each animal's spatial activity during a survey can be summarized by a fixed, but unknown, number of activity centers contained within a defined area (the state space). The observed and latent data are conditional on the number and location of these unobserved activity centers. Activity center locations are estimated as outcomes of a point process model within the state space that includes the survey grid extended by a buffer beyond the grid that is large enough to avoid detections of animals with activity centers outside the state space. Thus, $\hat{D}$ across the survey area is estimated from the number of activity centers in the state space that is estimated using spatiotemporal variation in detections of marked and unmarked animals (Chandler and Royle 2013; Royle et al. 2013).

For each model, we estimated the decline in detection probability with increasing distance from an animal's activity center using a hazard half-normal function. All spatial data were scaled to kilometers and then centered to reduce autocorrelation and improve mixing in the Markov chain Monte Carlo (MCMC) chains. The shape of the hazard half-normal function is defined by the parameters λ_0 and σ, which estimate the expected number of detections per sampling occasion at an animal's activity center and the inflection point of the half-normal curve, respectively. We estimated a single λ_0 and σ for each combination of site and species. In most cases, we used flat prior distributions for these parameters (λ_0, $\sigma = U(0, 5)$). We used a weak

prior ($\Gamma(8.65, 30)$; $\bar{x} = 0.29$ km, $SD = 0.10$) on σ for sambar deer populations at sites BL and CT to overcome difficulties with convergence. We based these weak priors on posterior distributions estimated from the same species at a similar site (GG; Supplementary Data SD2). We used between three and six MCMC chains for each model. Convergence and burn-in adequacy were assessed by examining trace plots, overlap of posterior distributions from each chain, and the Gelman–Rubin statistic $\hat{R}$ (Brooks and Gelman 1998). DA adequacy was assessed by visual checks for truncation in trace plots and posterior distributions. We used a series of short adaptation runs to tune the candidate distributions for λ_0 and σ so that the acceptance rates for these parameters were between 0.16 and 0.42. MCMC autocorrelation was usually still large after tuning, so all chains comprised ≥85,000 draws after discarding burn-ins to attain effective sample sizes >1,000 for posterior distributions for population density. At sites with a permeable boundary, we checked that the ratio of buffer size of the state space to σ was >3 so that we could be confident that animals with activity centers beyond the state space were not detected (Royle et al. 2013). We used the mean of the posterior distribution for the point estimate for $\hat{D}$ as posteriors were not heavily skewed.

To estimate the effects of variability in deer detections on precision, we used power functions to describe the effects of the number of unmarked detections, the number of marked individuals, and the number of recaptures of marked individuals on the CV of the $\hat{D}$ posterior mean: $CV = aX^b$. A negative b

parameter would indicate that CV decreased with increasing values of the predictor variable. The three predictor variables were all highly correlated ($r \geq 0.89$), so we used a separate model for each. Models were implemented in JAGS (Plummer 2003) called via the runjags package (Denwood 2016) in R, using three chains of 10,000 draws each after discarding 5,000 burn-in draws.

To summarize the detection data, we estimated the expected number of deer detections camera^{-1} day^{-1} using a Bayesian negative binomial random effects model, specifying camera station and day as random effects. Detection rate data such as these have been often used as indices of relative abundance for deer and other species and it is important to know how they vary with $\hat{D}$ (Parsons et al. 2017). For sambar deer, which was the only species with more than three density estimates, we used linear regression to estimate the relationship between the summary index values (on their original log scale) and the population density posterior modes. Models were implemented in JAGS as described previously.

All survey procedures were consistent with ASM guidelines for the use of live animals (Sikes and Animal Care and Use Committee of the American Society of Mammalogists 2016) and were approved by institutional animal welfare committees (ORA-18-21-016, Qld DAF CA2019/04/1281). The data and code used in our analyses are archived at Zenodo (Bengsen et al. 2021).

RESULTS

We surveyed for 23,955 camera days across the nine sites. The average number of deer detections camera^{-1} day^{-1} varied substantially among sites, ranging from 0.009 (95% credible interval (CrI) = 0.003, 0.019) for sambar deer at GG to 0.246 (95% CrI = 0.170, 0.351) for red deer at YY. The vast majority of detections could not be reliably assigned to an identifiable individual. The ratio of the number of marked to unmarked detections ranged from 0.03 to 0.28. We were able to reliably identify ≥ 2 individuals in each population, except for sambar deer at site SL where there was a total of five detections (Table 2). The

maximum distance between detections for any individual was 5,029 m for sambar and red deer at site YY. The mean distance between detections of individual marked deer ranged from 193 m for sambar deer at CD to 1,249 m for sambar deer at BL.

Twelve of the 13 combinations of site and species provided detection data that could be used in SMR models. There were insufficient detections of sambar deer at SL for modeling. On three occasions, we were unable to obtain satisfactory MCMC convergence after tuning and using weakly informative prior distributions. In these cases, we trimmed the detection histories to include only the middle 21 days to reduce the risk of sampling over unstable activity ranges. We then reverted to using flat priors (Table 2).

Estimated deer density ranged from 0.3 fallow deer km^{-2} at GG (95% CrI = 0.1, 0.5) to 24.6 red deer km^{-2} at SL (95% CrI = 19.8, 30.6; Table 3). Estimated baseline encounter rates (λ_0) were <0.02 at most sites but were much higher at two of the three sites for which we used 21-day detection history subsets (YP rusa λ_0 = 0.26, GG fallow λ_0 = 0.61). Half-normal scale parameter (σ) point estimates were all <1.0 km except for sambar deer at YY (1.36 km), suggesting that the upper limit of the prior distribution on σ (5 km) was adequate (Supplementary Data SD2).

Precision of the $\hat{D}$ posterior distribution increased (i.e., the CV decreased) with increasing numbers of marked individuals, recaptures, and unmarked detections. Increasing the number of marked individuals produced the most rapid decline in CV over the range of observed data (a = 0.70, b = −0.66) followed by increasing the number of recaptures (a = 1.06, b = −0.50) and increasing the number of unmarked detections (a = 16.96, b = −0.80; Fig. 4). For each model, the probability of a negative relationship between the CV and the independent variable (i.e., $b < 0$) was >0.99.

The sambar deer detection rate index increased with estimated density: ln(detections camera^{-1} day^{-1}) = −4.87 (95% CrI = −5.96, −3.71) + 0.25 (95% CrI = 0.05, 0.44) × $\hat{D}$ (R^2 = 0.84; Fig. 5). The probability of a positive relationship between the detection rate index and the posterior mean of $\hat{D}$ was >0.98.

Table 2.—Key data set and model characteristics used to estimate density of four deer species at nine sites. Nu is the number of deer detections that could not be assigned to a recognizable individuals, Nm is the number of detections of recognizable individuals, and r is the number of individual recaptures.

Deer species	Site	Camera days used	Nu	Nm	r	Mean group size	SE group size	Markov chain Monte Carlo draws used ('000s)	σ prior
Fallow	CD	3,141	141	4	14	1.37	0.55	1,470	$U(0, 5)$
Fallow	GG	819	123	2	4	1.23	0.45	981	$U(0, 5)$
Red	SL	1,198	309	20	61	2.55	0.88	1,458	$U(0, 5)$
Red	YY	3,177	1,263	43	151	1.90	0.74	870	$U(0, 5)$
Rusa	NP	735	68	4	11	1.28	0.55	1,470	$U(0, 5)$
Rusa	WD	2,486	382	5	32	1.32	0.54	4,471	$U(0, 5)$
Rusa	YP	756	68	3	7	1.47	0.63	1,171	$U(0, 5)$
Sambar	BL	3,306	119	4	19	1.16	0.36	1,310	$G(8.65, 30)$
Sambar	CD	3,141	587	8	20	1.35	0.50	834	$G(8.65, 30)$
Sambar	CT	2,429	67	2	21	1.14	0.33	661	$G(8.65, 30)$
Sambar	GG	3,268	186	8	42	1.23	0.54	1,111	$U(0, 5)$
Sambar	SL	1,198	5	0	0	1.30	0.59	NA	NA
Sambar	YY	3,177	159	7	21	1.37	0.55	870	$U(0, 5)$

Table 3.—Population density posterior summary statistics for four deer species at nine sites.

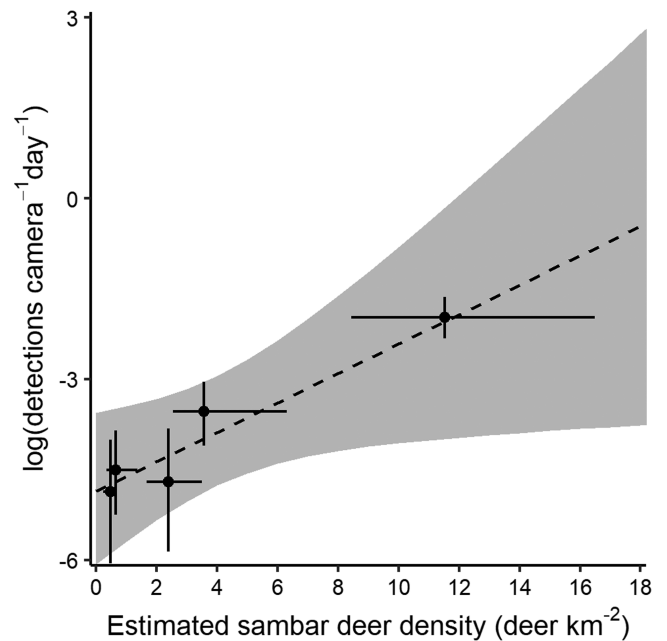| Species	Site	Mean	Mode	2.5% CrI	97.5% CrI	CV
Sambar	BL	0.73	0.64	0.33	1.35	0.36
Sambar	CD	11.94	11.53	8.44	16.48	0.17
Sambar	CT	0.48	0.41	0.24	0.84	0.32
Sambar	GG	2.49	2.38	1.67	3.50	0.19
Sambar	YY	3.93	3.56	2.53	6.29	0.25
Fallow	CD	2.09	1.95	1.46	2.92	0.17
Fallow	GG	0.29	0.25	0.12	0.53	0.36
Red	SL	24.57	24.05	19.79	30.64	0.11
Red	YY	19.76	19.64	17.58	22.17	0.06
Rusa	NP	3.11	2.78	1.76	5.07	0.27
Rusa	WD	10.34	9.93	7.84	13.32	0.13
Rusa	YP	0.68	0.42	0.21	1.77	0.61

CV = coefficient of variation, CrI = credible interval.
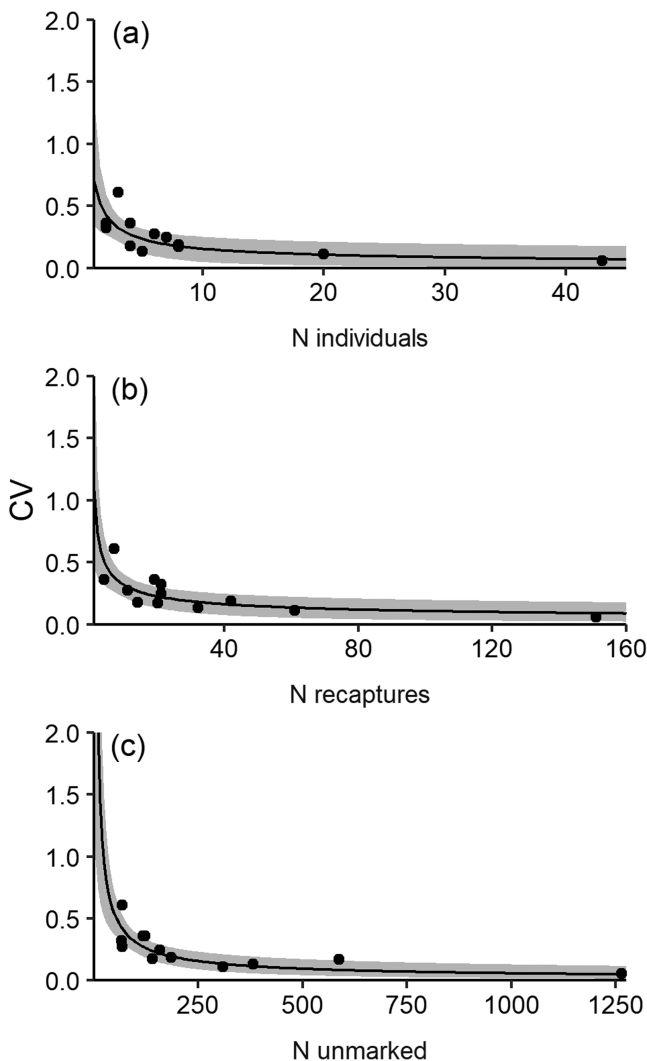
Fig. 4.—Effects of increasing numbers of (a) marked individuals, (b) recaptures of marked individuals, and (c) unmarked deer detections on the precision (coefficient of variation [CV]) of population density estimates. Shading shows the 95% credible interval for each function.

Fig. 5.—The detection rate index, calculated as ln(sambar detections camera^{-1} day^{-1}), increased with estimated population density (sambar deer km^{-2}). Solid lines represent 95% credible intervals of the estimates and the dashed line and shaded polygon show the predicted values and their 95% credible interval.

Discussion

This study has shown that camera trap data in which few individuals can be identified and recognized can be used with SMR models to estimate the population density of four deer species.

The diversity of study area shapes and sizes, environments (including tropical and temperate, coastal and high-elevation), deer populations, and camera grid characteristics in this study provided a robust evaluation of the approach and highlighted specific strengths and weaknesses that can be used to design more effective surveys to estimate deer density and abundance.

Specific strengths of the methods used here included: (i) the ability to estimate deer density in situations where more commonly used approaches such as transect-based animal counts are unsuitable; (ii) the favorable level of precision attained in most surveys; and (iii) the ability to incorporate prior information. We were able to estimate deer density in small, rugged, and densely vegetated sites and in seemingly low-density or cryptic populations that would be unlikely to provide sufficient numbers of detections for reliable estimation using transect-based animal counts. This is important for informing intensive management programs, such as eradication efforts, that often target

small geographic areas (e.g., sites CT, WD, YP) and low-density populations (e.g., Crouchley et al. 2011; Masters et al. 2018). It is particularly valuable when target populations inhabit densely vegetated terrain that is difficult to survey using visual counts of animals, as is often the case for sambar deer (Leslie 2011). A global systematic review of over 5,000 deer abundance and density estimates concluded that mark–recapture surveys using camera traps provided greater precision, on average (mean CV($\hat{D}$) = 0.39), than other survey methods for which sufficient data were available (Forsyth et al. 2022). Eleven of our 12 surveys provided greater precision than this average, with seven surveys attaining CV($\hat{D}$) ≤ 0.25. A final specific advantage of the methods used here was the ability to produce and exploit prior information on spatial detections. Use of a weakly informative prior distribution on σ derived from sambar deer detections at one site helped to achieve convergence in survey models for sambar deer at two other sites, without the prior information dominating the posterior distribution. Prior information for σ can also be derived from telemetry studies (e.g., Ramsey et al. 2015). The ability to use prior information should be most valuable for surveys in which spatial recaptures are sparse, such as surveys of low-density populations or surveys in which camera spacing provides poor coverage of deer movements.

Our SMR models performed well in most analyses, requiring little adjustment beyond tuning the candidate distributions to achieve acceptance rates that optimized effective sample size and computation time. Density estimates were within the range of expected values, given previous results from surveys of fallow deer (Bengsen et al. 2022), red deer (Amos et al. 2014), and rusa deer (Moriarty 2004b) in Australia and sambar deer in their native range (Karanth and Sunquist 1992; Khan et al. 1996). Two cases (sambar deer at BL and CT) benefited from weakly informative priors on σ that improved MCMC mixing, coverage, and posterior precision. In both cases, there was ≤10% overlap between the prior and the posterior distribution, indicating that the data were sufficiently informative to overcome the influence of the prior information (Gimenez et al. 2009). The strong positive relationships between precision and increasing numbers of marked individuals, individual recaptures, and unmarked detections were consistent with expectations from previous simulation studies (Chandler and Royle 2013; Royle et al. 2013; Efford and Boulanger 2019), highlighting the importance of sample size for precision.

Three of the four cases in which models required additional adjustment to attain convergence or provided low precision (CV > 0.35) had close camera spacing, relative to the observed movement patterns of deer. Camera spacing for fallow deer at GG, rusa deer at YP, and sambar deer at BL was less than σ, the detection function scale parameter. Simulation studies have shown that precision is often greatest at a camera spacing of 1.5σ to 2.5σ. Values in this range optimize the information available to estimate both the baseline encounter rate and the detection function by balancing the number of individuals captured, the number of recaptures, and the number and spatial distribution of spatial recaptures (Sollmann et al. 2012; Efford and Fewster 2013; Royle et al. 2013). At BL, the close camera spacing relative to σ was due to the unusually long distances between detections of individual sambar deer. A larger

survey grid with greater spacing between cameras might have improved precision at this site, provided it could increase the number of individuals captured without greatly reducing the number of spatial recaptures. However, greater camera spacing may not have been beneficial for estimating density of rusa deer at YP or fallow deer at GG. In both of these cases, deer detections were condensed within well-defined sections of the survey grid and showed little spatial variation across the full survey period. At YP, this was because the rusa deer population was only recently established and did not appear to have spread widely, whereas fallow deer detections at GG were restricted to low elevations within the site. Increasing the camera spacing at these sites would probably have led to a reduction in data available to estimate encounter rates and detection functions because fewer cameras would have been located in areas used by deer. Consequently, a greater camera spacing would probably have reduced the number of spatial recaptures without increasing the number of detections of marked or unmarked deer. In both cases, we trimmed the survey period to 21 days to reduce the risk that activity range centers were not stable during a long survey. This improved the mixing and stability of MCMC chains to an acceptable level. However, it also reduced the number of marked individuals, spatial recaptures, and unmarked detections. Consequently, precision of the baseline encounter rate and $\hat{D}$ for rusa deer at YP were poor (CV λ_0 = 0.45, CV $\hat{D}$ = 0.61), compared to other surveys in this study.

All but one of the 13 surveys in this study produced useful results. However, the need for weak priors for two surveys and trimming of the survey period for three surveys highlights the value of having an alternative method for estimating density and abundance. Abundance indices based on detection rates have been criticized for their inability to determine the extent to which changes in index value are attributable to variability in abundance or variability in detection probability (Anderson 2001; Sollmann et al. 2013b). Nonetheless, some camera-trapping studies have shown strong correlations between ungulate detection rates and densities estimated from the same data (Rovero and Marshall 2009; Parsons et al. 2017). The positive relationship between sambar deer detection rate and estimated density in the present study suggests that the detection rate index used here could be useful for identifying the direction of coarse changes in population state over a wide range of densities (0.5 to 11.5 sambar deer km^{-2}). Indices such as this are best suited to estimating changes in state when any differences in detection probabilities among surveys are likely to be heavily outweighed by differences in animal abundance, such as immediately before and after an intensive population control operation (Bengsen et al. 2014). Occupancy-based methods have also been popular for detecting differences among or within populations using camera trap data (e.g., Parsons et al. 2017; Schlichting et al. 2020), but the requirement for spatial independence among survey stations in occupancy surveys is inconsistent with the need for spatial dependence in SMR surveys.

Limitations.—The Bayesian SMR models used in this study provided a powerful and flexible tool for estimating deer densities across a wide range of situations that were not amenable to more commonly used methods such as transect-based

counts of deer or their sign. However, effective use and adaptation of these models requires a level of working knowledge that can take a considerable commitment of time and effort to develop. Many wildlife managers wishing to use these methods may need to partner with collaborators who already have, or can acquire, the necessary expertise. Further, survey design constraints meant that the approach was best suited to situations in which the survey area was modest in size and results were not required urgently. The survey area constraint was imposed by the need for camera spacing to be small enough to provide spatial recaptures. The timeliness constraint was imposed by the long duration of surveys and the time taken to process camera trap images and run models.

Using the average σ estimate from our surveys of 0.54 km, a contiguous hexagonal survey grid comprising 33 camera stations could cover 33 km^2 at a camera spacing of 2σ. This is small, relative to the scale of 100s of km^2 that can be covered by aerial survey, for example (Forsyth et al. 2022). Hierarchical survey designs that use clusters of camera stations such that spatial recaptures can occur within widely spaced groups of cameras could extend the spatial area sampled by survey grids (Efford and Fewster 2013; Sun et al. 2014). Optimization criteria and functions are available to help predict the most informative detector station layouts for a given survey area (Dupont et al. 2021).

The time constraint could be reduced in some cases by shortening the survey duration. Three surveys produced results using 21-day survey periods, although precision was lower than all but one of the other surveys which ranged from 64 to 109 days. An optimal survey duration would be long enough to collect and exploit as much detection data as possible while being short enough to maintain demographic and geographic population closure (Royle et al. 2013). Processing many thousands of camera trap images and carefully identifying individuals is also time-consuming and expensive. Machine-learning algorithms are being developed to assist with identifying different species and individuals in camera trap images (Schneider et al. 2019; Tabak et al. 2019; Meek et al. 2020).

A further limitation of our surveys was the need to discard data from individuals that could be clearly identified on some occasions, but whose markings were not sufficiently obvious to allow them to be identified with certainty every time that they were photographed. Including these detections as marked individuals would have led to underestimation of detection probability and overestimation of density, so they were counted as only unmarked detections. Including detections with ambiguous markings would also reduce repeatability due to inconsistencies among observers. This might have been partially overcome by using paired cameras that photographed both flanks of animals simultaneously (Karanth et al. 2011), although this would have increased deployment and processing costs. White-flash cameras capable of recording greater information content from detections in low light could also have been used, but this may have increased the risks of aversive responses from deer (Henrich et al. 2020) and theft of cameras by people. Alternatively, latent identities of detections that were observed to bear markings without being conclusively identifiable could be estimated and assigned using a probabilistic spatial submodel (Augustine et al. 2018; Whittington et al. 2018; Murphy et al. 2019). However, the presence of natural markings that could not be used in the present surveys, such as ear notches or scarring on a single flank, was often ambiguous.

Recommendations.—Camera trap surveys for estimating deer density using SMR models should be designed to provide data that can promote model convergence and produce a level of precision that is suitable for the aims of the study. In practice, this will often mean maximizing precision, given a fixed level of survey effort. Our results showed that the numbers of marked individuals, recaptures of marked individuals, and unmarked detections were all important contributors to the precision of density estimates. Based on our experiences and results across 12 combinations of site and deer species, we offer the following general survey design and implementation recommendations which aim to improve the likelihood of models achieving convergence and good precision under a wide range of conditions:

1) Survey design should make full use of existing information on the likely spatial distribution, movement patterns, and detection probabilities of the target species. Ideally, such information would be derived from a local pilot study (Kristensen and Kovach 2018), but it could also be drawn from previous studies in other areas.

2) A 90-day survey period should often provide a balance of sample size, activity range stability, timeliness of results, and flexibility to subset the data. Our cameras were deployed for between 64 and 109 days which provided the opportunity to collect useful sample sizes. In three cases, the full survey duration may have been too long to ensure population closure or stability of activity ranges. However, we were able to use a subset of data from the full survey period for analysis, whereas a survey cannot usually be extended once the data have been collected and found to be insufficient.

3) Surveys should be conducted during periods when spatial behavior is most likely to be stable. Long periods of spatial stability provide the greatest opportunity for long surveys and favorable sample sizes without violating the assumptions that the population is geographically closed and activity range centers are stable. Many deer species and populations experience predictable periods of spatial instability such as rutting, migration, and birthing seasons (e.g., Perelberg et al. 2003; Sawyer et al. 2005; Ciuti et al. 2006) that should be avoided. Birthing seasons should also be avoided to avoid violating demographic closure, as should periods of predictably high mortality, such as harsh winters or intense hunting seasons.

4) In the absence of site-specific prior information, a minimum of 30 cameras is desirable, but surveys should use as many cameras as practicable to ensure good spatial coverage and sample size. All of our surveys that used at least 29 camera stations achieved acceptable results. One survey using 12 camera stations also achieved good results in a small, insular site with a high-density red deer population that provided a large sample size, despite the

small effort. However, the same survey grid provided insufficient data to estimate the density of a sparser sambar deer population constrained within the same site.

5) Camera spacing should reflect expected values of σ. Camera spacings of 1.5σ to 2σ are often considered desirable for spatial capture–recapture studies (Efford and Boulanger 2019) and this should hold for SMR models. However, when detection probabilities are low, as was often the case in our surveys (mean $\lambda_0 = 0.10 \pm SD$ 0.17), a camera spacing < σ may provide greater precision (Kristensen and Kovach 2018). For some species, ranges of expected values of σ can often be estimated from telemetry data or from the results of the present study, although results from local camera trap surveys will usually be preferable. Given the range of σ estimates from our surveys, a camera spacing between 500 and 1,000 m should often provide an optimal balance of numbers of individuals and numbers of spatial recaptures. Combinations of camera numbers and spacing that produce survey grid extents much smaller than the size of animal activity ranges cannot be expected to provide reliable results (Sollmann et al. 2012; Efford and Boulanger 2019).

6) Spatial clustering or irregular distribution of cameras should be considered when the number of cameras and suggested spacing are insufficient to cover the area of interest. We did not evaluate this in the present study, but sambar deer density estimation at site BL may have benefited from this approach. Clustered survey designs can increase the area covered by a camera trap survey and the number of individuals detected without biasing spatial capture–recapture parameter estimates (Sun et al. 2014; Efford and Boulanger 2019; Dupont et al. 2021). The optimal allocation of effort across cluster size and number of clusters can be explored using optimization algorithms and simulations (Sun et al. 2014; Efford and Boulanger 2019; Dupont et al. 2021).

Conclusion

Our study shows that SMR models can be used with camera trap grids to estimate the density and abundance of deer. The method provided precise and biologically plausible estimates of abundance for four deer species at most of the nine sites we surveyed in eastern Australia. The diversity of deer species (two temperate, two tropical) and study areas suggests that the method has wide application globally. The models are extremely flexible, accommodating populations in which all, some or no individuals are recognizable. In the absence of specific local information on deer detectability and movement patterns, and assuming similar detection rates as those estimated across our study sites and species, we recommend that at least 30 cameras be spaced at 500–1,000 m and set for 90 days.

Acknowledgments

Funding

Supplementary Data

Supplementary data are available at *Journal of Mammalogy* online.

Supplementary Data SD1.—Density plots of time differences between successive camera triggers caused by four deer species at nine sites.

Supplementary Data SD2.—Posterior summary statistics for spatial mark–resight parameters.

Literature Cited

Amos M., Baxter G., Finch N., Lisle A., Murray P. 2014. I just want to count them! Considerations when choosing a deer population monitoring method. Wildlife Biology 20:362–370.

Anderson D.R. 2001. The need to get the basics right in wildlife field studies. Wildlife Society Bulletin 29:1294–1297.

Augustine B.C., Royle J.A., Kelly M.J., Satter C.B., Alonso R.S., Boydston E.E. Crooks K.R.. 2018. Spatial capture–recapture with partial identity: an application to camera traps. The Annals of Applied Statistics 12:67–95.

Bengsen A.J., Forsyth D.M., Ramsey D.S.L., Amos M., Brennan M., Pople A. 2021. AndrewBengsen/wild deer spatial mark-resight models and data. Zenodo. doi:10.5281/zenodo.4849263.

Bengsen A.J., et al. 2022. AndrewBengsen/Helicopter-based-shooting-of-deer_revised. Zenodo. doi:10.5281/zenodo.6070097.

Bengsen A.J., Hampton J.O., Comte S., Freney S., Forsyth D.M. 2021. Evaluation of helicopter net-gunning to capture wild fallow deer (*Dama dama*). Wildlife Research 48:722–729.

Bengsen A.J., Robinson R., Chaffey C., Gavenlock J., Hornsby V., Hurst R., Fosdick M. 2014. Camera trap surveys to evaluate pest animal control operations. Ecological Management & Restoration 15:97–100.

Brooks S.P., Gelman A. 1998. General methods for monitoring convergence of iterative simulations. Journal of Computational and Graphical Statistics 7:434–455.

Chandler R.B., Royle J.A. 2013. Spatially explicit models for inference about density in unmarked or partially marked populations. The Annals of Applied Statistics 7:936–954.

Ciuti S., Bongi P., Vassale S., Apollonio M. 2006. Influence of fawning on the spatial behaviour and habitat selection of female fallow deer (*Dama dama*) during late pregnancy and early lactation. Journal of Zoology 268:97–107.

Crouchley D., Nugent G., Edge K. 2011. Removal of red deer (*Cervus elaphus*) from Anchor and Secretary Islands, Fiordland, New Zealand. In: Veitch C.R., Clout M.N., Towns D.R., editors. Island invasives: eradication and management. IUCN, Gland, Switzerland; p. 422–425.

Davis N.E., Bennett A., Forsyth D.M., Bowman D.M.J.S., Lefroy E.C., Wood S.W., Woolnough A.P., West P., Hampton J.O., Johnson C.N. 2016. A systematic review of the impacts and management of introduced deer (family Cervidae) in Australia. Wildlife Research 43:515–532.

Denwood M.J. 2016. runjags: an R package providing interface utilities, model templates, parallel computing methods and additional distributions for MCMC models in JAGS. Journal of Statistical Software 71:1–25.

Dupont P., Milleret C., Gimenez O., Bischof R. 2019. Population closure and the bias-precision trade-off in spatial capture–recapture. Methods in Ecology and Evolution 10:661–672.

Dupont G., Royle J.A., Nawaz M.A., Sutherland C. 2021. Optimal sampling design for spatial capture-recapture. Ecology 102:e03262.

Efford M.G., Boulanger J. 2019. Fast evaluation of study designs for spatially explicit capture–recapture. Methods in Ecology and Evolution 10:1529–1535.

Efford M.G., Fewster R.M. 2013. Estimating population size by spatially explicit capture–recapture. Oikos 122:918–928.

Evans M.J., Rittenhouse T.A. 2018. Evaluating spatially explicit density estimates of unmarked wildlife detected by remote cameras. Journal of Applied Ecology 55:2565–2574.

Forsyth D.M., Comte S., Davis N.E., Bengsen A.J., Mysterud A., Côté S.D., Hewitt D.G., Morellet N. 2022. Methodology matters when estimating deer abundance: a global systematic review and recommendations for improvements. Journal of Wildlife Management (in press).

Forsyth D.M., Ramsey D.S., Woodford L.P. 2019. Estimating abundances, densities, and interspecific associations in a carnivore community. Journal of Wildlife Management 83:1090–1102.

Gardner P.C., Vaughan I.P., Liew L.P., Goossens B. 2019. Using natural marks in a spatially explicit capture-recapture framework to estimate preliminary population density of cryptic endangered wild cattle in Borneo. Global Ecology and Conservation 20:e00748.

Gimenez O., Morgan B.J.T., Brooks S.P. 2009. Weak identifiability in models for mark-recapture-recovery data. In: Thomson D.L., Cooch E.G., Conroy M.J. editors. Modeling demographic processes in marked populations. Springer, Boston, Massachusetts, USA; p. 1055–1067.

Hampton J.O., ET AL. 2019. A review of methods used to capture and restrain introduced wild deer in Australia. Australian Mammalogy 41:1–11.

Henrich M., Niederlechner S., Kröschel M., Thoma S., Dormann C.F., Hartig F., Heurich M. 2020. The influence of camera trap flash type on the behavioural reactions and trapping rates of red deer and roe deer. Remote Sensing in Ecology and Conservation 6:399–410.

Hewitt D.G. 2011. Biology and management of white-tailed deer. CRC Press, Boca-Raton, Florida, USA.

Jiménez J., Higuero R., Charre-Medellin J.F., Acevedo P. 2017. Spatial mark-resight models to estimate feral pig population density. Hystrix 28:208–213.

Kane M.D., Morin D.J., Kelly M.J. 2015. Potential for camera-traps and spatial mark-resight models to improve monitoring of the critically endangered West African lion (*Panthera leo*). Biodiversity and Conservation 24:3527–3541.

Karanth K.U., Nichols J.D., Kumar N.S. 2011. Estimating tiger abundance from camera trap data: field surveys and analytical issues. In: O'Connell A.F., Nichols J.D., Karanth K.U., editors. Camera traps in animal ecology: methods and analyses. Springer, Tokyo; p. 97–117.

Karanth K.U., Sunquist M.E. 1992. Population structure, density and biomass of large herbivores in the tropical forests of Nagarahole, India. Journal of Tropical Ecology 8:21–35.

Khan J.A., Chellam R., Rodgers W.A., Johnsingh A.J.T. 1996. Ungulate densities and biomass in the tropical dry deciduous forests of Gir, Gujarat, India. Journal of Tropical Ecology 12:149–162.

Kowalski M., Kowalski M. 2013. ExifPro photo browser v 2.1.0. http://www.exifpro.com/ accessed 28 September 2017.

Kristensen T.V., Kovach A.I. 2018. Spatially explicit abundance estimation of a rare habitat specialist: implications for SECR study design. Ecosphere 9:e02217.

Leslie D.M. 2011. *Rusa unicolor* (Artiodactyla: Cervidae). Mammalian Species 43:1–30.

Macaulay L.T., Sollmann R., Barrett R.H. 2019. Estimating deer populations using camera traps and natural marks. The Journal of Wildlife Management 84:301–310.

Martins R.F., Schmidt A., Lenz D., Wilting A., Fickel J. 2018. Human-mediated introduction of introgressed deer across Wallace's line: historical biogeography of *Rusa unicolor* and *R. timorensis*. Ecology and Evolution 8:1465–1479.

Masters P., Markopoulos N., Florance B., Southgate R. 2018. The eradication of fallow deer (*Dama dama*) and feral goats (*Capra hircus*) from Kangaroo Island, South Australia. Australasian Journal of Environmental Management 25:86–98.

Mattioli S. 2011. Family Cervidae (deer). In: Wilson D., Mittermeier R., editors. Handbook of the mammals of the world. Lynx Edicions, Barcelona, Spain; p. 350–443.

McShea W.J., Underwood H.B., Rappole J.H. 1996. The science of overabundance: deer ecology and population management. Smithsonian Institution Press, Washington, District of Columbia, USA.

Meek P.D., Ballard G., Falzon G., Williamson J., Milne H., Farrell R., Stover J., Mather-Zardain A.T., Bishop J.C., Cheung E.K.W. 2020. Camera trapping technology and related advances: into the new millennium. Australian Zoologist 40:392.

Moriarty A.J. 2004a. The liberation, distribution, abundance and management of wild deer in Australia. Wildlife Research 31:291–299.

Moriarty A.J. 2004b. Ecology and environmental impact of Javan rusa deer (*Cervus timorensis russa*) in the Royal National Park. Dissertation, University of Western Sydney, Penrith, Australia.

Murphy S.M., Wilckens D.T., Augustine B.C., Peyton M.A., Harper G.C. 2019. Improving estimation of puma (*Puma concolor*) population density: clustered camera-trapping, telemetry data, and generalized spatial mark-resight models. Scientific Reports 9:1–13.

Niedballa J., Sollmann R., Courtiol A., Wilting A. 2016. camtrapR: an R package for efficient camera trap data management. Methods in Ecology and Evolution 7:1457–1462.

Parsons A.W., Forrester T., McShea W.J., Baker-Whatton M.C., Millspaugh J.J., Kays R. 2017. Do occupancy or detection rates

from camera traps reflect deer density? Journal of Mammalogy 98:1547–1557.

Perelberg A., Saltz D., Bar-David S., Dolev A., Yom-Tov Y. 2003. Seasonal and circadian changes in the home ranges of reintroduced Persian fallow deer. The Journal of Wildlife Management 67:485–492.

Plummer M. 2003. JAGS: a program for analysis of Bayesian graphical models using Gibbs sampling. In: Hornik K., Leisch F., Zeileis A., editors. Proceedings of the 3rd International Workshop on Distributed Statistical Computing; 20–23 March 2003; Vienna, Austria. Technische Universität Wien; p. 1–8.

R Core Team. 2020. R: a language and environment for statistical computing, Version 3.6.2. R Foundation for Statistical Computing, Vienna, Austria. www.R-project.org/. Accessed 17 January 2020.

Ramsey D.S.L., Caley P.A., Robley A. 2015. Estimating population density from presence–absence data using a spatially explicit model. The Journal of Wildlife Management 79:491–499.

Rich L.N., Kelly M.J., Sollmann R., Noss A.J., Maffei L., Arispe R.L., Paviolo A., De Angelo C.D., Di Blanco Y.E., Di Bitetti M.S. 2014. Comparing capture-recapture, mark-resight, and spatial mark-resight models for estimating puma densities via camera traps. Journal of Mammalogy 95:382–391.

Rovero F., Marshall A.R. 2009. Camera trapping photographic rate as an index of density in forest ungulates. Journal of Applied Ecology 46:1011–1017.

Royle J.A., Chandler R.B., Sollmann R., Gardner B. 2013. Spatial capture-recapture. Academic Press, Waltham, Massachusetts, USA.

Sawyer H., Lindzey F., McWhirter D. 2005. Mule deer and pronghorn migration in western Wyoming. Wildlife Society Bulletin 33:1266–1273.

Schlichting P.E., Beasley J.C., Boughton R.K., Davis A.J., Pepin K.M., Glow M.P., Snow N.P., Miller R.S., VerCauteren K.C., Lewis J.S. 2020. A rapid population assessment method for wild pigs using baited cameras at 3 study sites. Wildlife Society Bulletin 44:372–382.

Schneider S., Taylor G.W., Linquist S., Kremer S.C. 2019. Past, present and future approaches using computer vision for animal re-identification from camera trap data. Methods in Ecology and Evolution 10:461–470.

Sikes R.S., and The Animal Care and Use Committee of the American Society of Mammalogists. 2016. 2016 Guidelines of the American Society of Mammalogists for the use of wild mammals in research and education. Journal of Mammalogy 97:663–688.

Skalski J.R., Ryding K.E., Millspaugh J. 2005. Wildlife demography: analysis of sex, age, and count data. Elsevier Academic Press, Burlington, Massachusetts, USA.

Sollmann R., Gardner B., Belant J.L. 2012. How does spatial study design influence density estimates from spatial capture-recapture models? PLoS One 7:e34575.

Sollmann R., Gardner B., Parsons A.W., Stocking J.J., McClintock B.T., Simons T.R., Pollock K.H., O'Connell A.F. 2013a. A spatial mark–resight model augmented with telemetry data. Ecology 94:553–559.

Sollmann R., Mohamed A., Samejima H., Wilting A. 2013b. Risky business or simple solution—relative abundance indices from camera-trapping. Biological Conservation 159:405–412.

Sun C.C., Fuller A.K., Royle J.A. 2014. Trap configuration and spacing influences parameter estimates in spatial capture-recapture models. PLoS One 9:e88025.

Tabak M.A., Norouzzadeh M.S., Wolfson D.W., Sweeney S.J., VerCauteren K.C., Snow N.P., Halseth J.M., Di Salvo P.A., Lewis J.S., White M.D. 2019. Machine learning to classify animal species in camera trap images: applications in ecology. Methods in Ecology and Evolution 10:585–590.

Whittington J., Hebblewhite M., Chandler R.B. 2018. Generalized spatial mark–resight models with an application to grizzly bears. Journal of Applied Ecology 55:157–168.

Williams B.K., Nichols J.D., Conroy M.J. 2002. Analysis and management of animal populations: modeling, estimation, and decision making. Academic Press, San Diego, California, USA.